HHS Public Access

Author manuscript

Sci Transl Med. Author manuscript; available in PMC 2021 July 06.

Published in final edited form as:

Sci Transl Med. 2021 January 06; 13(575): . doi:10.1126/scitranslmed.abb6295.

Reversible ON- and OFF-switch chimeric antigen receptors controlled by lenalidomide

Max Jan[1,2,3], **Irene Scarfò**[4], **Rebecca C Larson**[4], **Amanda Walker**[1,2,5], **Andrea Schmidts**[4], **Andrew A Guirguis**[1,2], **Jessica A Gasser**[1,2], **Mikołaj Słabicki**[1,2], **Amanda A Bouffard**[4], **Ana P Castano**[4], **Michael C Kann**[4], **Maria L Cabral**[4], **Alexander Tepper**[1,2], **Daniel E Grinshpun**[1,2], **Adam S Sperling**[1,2], **Taeyoon Kyung**[6], **Quinlan Sievers**[1], **Michael E Birnbaum**[6], **Marcela V Maus**[1,4,*], **Benjamin L Ebert**[1,2,7,*]

[1]Broad Institute of Harvard and MIT, Cambridge, MA 02142, USA

[2]Dana-Farber Cancer Institute, Department of Medical Oncology, Boston, MA 02215, USA

[3]Department of Pathology, Massachusetts General Hospital, Boston, MA 02114, USA

[4]Cellular Immunotherapy Program, Massachusetts General Hospital Cancer Center, Charlestown, MA and Harvard Medical School, Boston 02114, MA

[5]Sidney Kimmel Medical College at Thomas Jefferson University, Philadelphia, PA 19107, USA

[6]Department of Biological Engineering, Massachusetts Institute of Technology, Cambridge, MA 02142, USA

[7]Howard Hughes Medical Institute, Dana-Farber Cancer Institute, Boston, MA 02215, USA

Abstract

Cell-based therapies are emerging as effective agents against cancer and other diseases. As autonomous “living drugs,” these therapies lack precise control. Chimeric antigen receptor (CAR) T cells effectively target hematologic malignancies but can proliferate rapidly and cause toxicity. We developed ON and OFF switches for CAR T cells using the clinically approved drug lenalidomide, which mediates the proteasomal degradation of several target proteins by inducing interactions between the $CRL4^{CRBN}$ E3 ubiquitin ligase and a C2H2 zinc finger degron motif. We performed a systematic screen to identify “super-degron” tags with enhanced sensitivity to lenalidomide-induced degradation and used these degradable tags to generate OFF-switch degradable CARs. To create an ON switch, we engineered a lenalidomide-inducible dimerization system and developed split CARs that required both lenalidomide and target antigen for activation. Subtherapeutic lenalidomide concentrations controlled the effector functions of ON- and OFF-switch CAR T cells. In vivo, ON-switch split CARs demonstrated lenalidomide-dependent anti-tumor activity, and OFF-switch degradable CARs were depleted by drug treatment to limit

Correspondence: Marcela V. Maus, 149 13th St, Room 3.216, Charlestown, MA 02129; mvmaus@mgh.harvard.edu, and Benjamin L. Ebert, Dana-Farber Cancer Institute, 450 Brookline Ave, D1610A, Boston, MA 02215; benjamin_ebert@dfci.harvard.edu.

*Contributed equally

Author contributions:

M.J., I.S., R.C.L., A.S., Q.S., A.S.S., T.K., M.E.B., M.V.M., B.L.E., designed research studies; M.J., A.W., A.A.G., J.A.G., A.A.B., A.P.C., M.C.K., M.L.C., A.T., and D.E.G., acquired data; M.J. and M.S. analyzed data; M.J., M.V.M., and B.L.E. wrote and edited the manuscript.

inflammatory cytokine production while retaining anti-tumor efficacy. Together, the data showed that these lenalidomide-gated switches are rapid, reversible, and clinically suitable systems to control transgene function in diverse gene- and cell-based therapies.

One sentence summary:

Two chemical genetic control systems were engineered to regulate CAR T cell function with lenalidomide.

Introduction

Genetically-engineered cell-based therapies are emerging as transformative agents against cancer, autoimmune disease, and monogenetic disorders (1, 2). These therapies are complicated by variable pharmacokinetics and effector functions (3). For example, the population of T cells genetically retargeted with chimeric antigen receptors (CARs) against tumor-associated antigens, such as CD19, dramatically expands and contracts in patients in response to antigen. The profound clinical successes of CAR T cell therapies targeting relapsed or refractory B cell malignancies have been achieved in spite of the risk of toxicity from T cell hyperactivation syndromes (4, 5). However, in some patient populations, such as adults with acute lymphoblastic leukemia, the toxicities associated with CAR T cells have stalled further clinical development, despite early signs of efficacy (6, 7). Control systems have the potential to improve the safety, efficacy, and accessibility of future cell-based therapies.

Chemical genetic control of protein stability enables rapid perturbation of biologic processes (8). Multiple systems now exist to regulate protein degradation, including the incorporation of destabilization domains (9), or sequences triggering auxin-induced degradation (10), ligand-induced degradation (11), and small molecule-assisted shutoff (12), or dTags (13). Although these systems are invaluable research tools and models for future cell-based therapies, there is a clinical need for chemical genetic control systems that are engineered from non-immunogenic human polypeptide sequences, are controlled by FDA-approved and non-immunosuppressive drugs, and afford robust ON- and OFF-switch control of protein stability. To satisfy each of these principles of clinical suitability, we endeavored to create control systems gated by thalidomide analogs for cell-based therapies.

Thalidomide, lenalidomide, and pomalidomide are effective and clinically approved therapies for multiple myeloma, subtypes of non-Hodgkin lymphoma, and myelodysplastic syndrome with chromosome 5q deletion. Thalidomide analogs act as molecular glues, bridging interactions between the $CRL4^{CRBN}$ E3 ubiquitin ligase and disease-relevant proteins that are subsequently ubiquitinated and degraded by the proteasome, resulting in therapeutic efficacy (14–16). Lenalidomide and pomalidomide are structurally related analogs in broad clinical use; pomalidomide has clinical efficacy in patients with multiple myeloma refractory to lenalidomide, which is largely explained by more effective degradation of a nearly identical range of substrate proteins (17, 18). A set of Cys2-His2 (C2H2) zinc fingers is a recurrent degron motif mediating drug-dependent interactions with $CRL4^{CRBN}$ (18–21). We hypothesized that these small, modular, human C2H2 zinc finger

domains could be engineered and repurposed to induce drug-dependent OFF-switch depletion of engineered proteins. Further, for ON-switch control, we hypothesized that the CRBN-thalidomide analog-zinc finger ternary interaction could be uncoupled from the ubiquitin-proteasome system to generate a stable lenalidomide-inducible dimerization system.

As proof of concept for cell-based therapies controlled by lenalidomide-gated switches, we engineered chemically controllable systems into CARs to address an unmet clinical need. Although demonstrating remarkable efficacy culminating in clinical approvals for the treatment of B cell acute lymphoblastic leukemia and diffuse large B cell lymphoma (22), CARs pose a risk from toxic T cell hyperactivation (23). Whereas the current management of cytokine release and immune cell-associated neurologic syndromes consists of supportive care, tocilizumab, with or without high-dose corticosteroids (4), we propose that these hyperactivation syndromes would be more easily managed if clinicians could rapidly and reversibly control CAR degradation and signaling. Here, we report the engineering of two chemical genetic control systems gated by lenalidomide, with proof of concept application to CAR T cells.

Results

Design of lenalidomide OFF-switch degradable CARs and ON-switch split CARs

We designed an OFF switch triggered by lenalidomide-induced CAR degradation (Fig. 1A). CAR T cells are engineered to activate upon recognition of a target tumor antigen. To turn off CAR signaling, lenalidomide (or another thalidomide analog) would induce $CRL4^{CRBN}$-mediated ubiquitination and proteasomal degradation (24) of the degron-tagged CAR. As levels of the small molecule controller fall, translation of CAR protein restores CAR signaling.

To test whether transmembrane receptors incorporating a lenalidomide-dependent degron tag were depleted from the cell surface, we engineered Jurkat T cells expressing either a CAR with an extracellular domain that recognizes CD19, a single transmembrane domain, and intracellular signaling domains from 4–1BB and CD3z (“conventional” CAR) or the same CAR plus the lenalidomide-dependent degron from IKZF3 (18) as a C-terminal tag. Whereas conventional CAR expression was insensitive to lenalidomide, the degradable CAR was depleted 14-fold from baseline (absence of lenalidomide) after incubation with 1 μM lenalidomide (Fig. 1B), supporting the use of targeted protein degradation for posttranslational regulation of CAR abundance.

We next designed an ON switch mediated by lenalidomide-inducible dimerization to control a two-component split CAR (Fig. 1C). In this construct, one subunit of the CAR included the CD19 recognition domain, CD28 transmembrane and intracellular signaling domains along with the lenalidomide-dependent zinc finger from IKZF3. The other subunit included CD8 alpha hinge and transmembrane domains, a CD28 domain, a mutated CRBN, and a CD3z signaling domain. As a model for T cell activation, Jurkat T cells expressing conventional or split CARs were evaluated for the percent of cells positive for the early activation marker CD69 (25) after co-culture with K562 target cells transduced to express

CD19 or empty vector and treatment with either lenalidomide or vehicle control. CD19-dependent activation of the conventional CAR T cells was insensitive to lenalidomide. However, CD19-dependent activation of the split CAR T cells was increased by 5-fold with lenalidomide, supporting the use of lenalidomide-inducible dimerization as an ON switch to regulate CAR T cell activation (Fig. 1D).

To design the lenalidomide-inducible dimerization, we reasoned that variants of CRBN and IKZF3 could be engineered so that their ternary interaction with lenalidomide no longer results in degradation. Within the $CRL4^{CRBN}$ E3 ubiquitin ligase complex, the substrate adapter DDB1 mediates the interaction with the substrate receptor CRBN. Crystallographic analyses of complexes containing DDB1, CRBN, and a thalidomide analog indicate that the domain of CRBN responsible for neosubstrate and drug binding is separate from the domain of CRBN that interacts with DDB1 (26–28). Thus, we hypothesized that the DDB1-binding domain within CRBN is dispensable for drug-induced interactions with substrate proteins such as IKZF3. Indeed, CRBN variants lacking the DDB1-binding domain exhibited a pomalidomide-dependent interaction with a fragment of IKZF3 in bioluminescence resonance energy transfer (BRET) cellular proximity-based assays (Fig. 2A). CRBNΔ3 was the variant with the strongest pomalidomide dependency for IKZF3 interaction. Ligand-inducible proximity was enhanced by incorporation of CRBNΔ3 and the IKZF3 degron fragment into cell surface-localized components of a split CAR (29, 30), in which antigen-binding and signaling domains are encoded in separate proteins (Fig. 2B). To protect from degradation by endogenous $CRL4^{CRBN}$ following exposure to lenalidomide, all intracellular lysine residues in the IKZF3 and adjacent CD28 costimulatory domain were replaced with arginine residues, which further enhanced the signal in the induced-proximity system (Fig. 2C). In summary, an E3 ubiquitin ligase-molecular glue-substrate ternary interaction was converted into a lenalidomide-inducible dimerization system for ON-switch regulation of a split CAR.

A hybrid zinc finger screen identifies super-degrons

Although the IKZF3-based degradation and dimerization switches demonstrated efficacy at drug concentrations that are used therapeutically, we sought to engineer more sensitive synthetic components that could act at subtherapeutic drug concentrations to minimize other effects of the thalidomide analogs. Multiple zinc fingers in human proteins are individually capable of mediating drug-dependent degradation at different efficiencies (18, 20). We hypothesized that zinc finger domains could be engineered to mediate drug-dependent degradation more efficiently than any present in the human proteome (hereafter termed “super-degrons”). We created a library composed of all possible N-terminal beta-hairpin and C-terminal alpha-helix combinations from 22 C2H2 zinc fingers that we previously determined to mediate thalidomide analog-dependent binding to CRBN (18) and encoded this library into a lentiviral degradation reporter vector wherein the zinc finger is tagged to enhanced green fluorescent protein (eGFP) and followed by an internal ribosome entry site (IRES)-mCherry element (18). The ratio of tagged eGFP to untagged mCherry fluorescence indicates zinc finger degradation status.

To screen for the synthetic zinc fingers that mediate drug-dependent degradation most efficiently, we transduced Jurkat T cells with the hybrid zinc finger library and then treated the cells with vehicle control or a thalidomide analog: lenalidomide, pomalidomide, avadomide, or iberdomide (Fig. 3A). Fluorescence-activated cell sorting (FACS) was used to isolate cells depleted of GFP-tagged zinc fingers (Fig. 3B), and the relative frequency of individual zinc fingers was quantified by next-generation sequencing (data file S1). Zinc fingers demonstrating drug-dependent degradation were enriched in drug-treated versus control-treated $eGFP^{low}$ populations. With lenalidomide, the 21 most enriched zinc fingers were hybrid forms, and 20 of these 21 candidate super-degrons were composed from the matrix of 5 N-termini (ZN653, ZN827, ZFP91, ZN276, IKZF3) with 7 C-termini (ZN787, ZN517, IKZF3, ZN654, PATZ1, E4F1, and ZKSC5) (Fig. 3C). Similar findings were identified for pomalidomide (fig. S1), avadomide (fig. S2), and iberdomide (fig. S3). The preferred N-terminal beta-hairpins converged on a similar sequence containing residues with crystallographic evidence of side chain-drug interactions (18) but were otherwise molecularly diverse (Fig. 3D). Through this analysis, we identified a group of zinc finger subdomains that promiscuously combine to form lenalidomide-dependent hybrid super-degrons more efficiently degraded than their parent zinc fingers.

To characterize individual super-degrons suited for synthetic biology applications, we investigated 6 hybrid zinc fingers in further detail. We transduced Jurkat cells to express each of the 6 hybrid and 8 associated parent zinc fingers and subjected the cells to a range of doses of lenalidomide, pomalidomide, avadomide, and iberdomide. The ZN653-PATZ1 hybrid, for example, demonstrates more efficient pomalidomide-dependent degradation than either parent zinc finger (fig. S4A). The half maximal degradation concentration (DC50) by lenalidomide or pomalidomide was lower for the 6 hybrid zinc fingers than for the corresponding parent zinc fingers (fig. S4B). Because the flanking sequence around the IKZF1 zinc finger degron augments affinity for CRBN-pomalidomide (18), we tested degrons extended by 60 amino acids to optimize the efficiency of our candidate super-degrons (Fig. 3E–G). In this extended format, the DC50 of the most efficient super-degrons was 2 – 6-times lower than that of the native IKZF3 degron across the tested thalidomide analogs. Among several comparable sequences, we chose ZFP91-IKZF3 for further study in both ON- and OFF-switch CARs.

A hybrid zinc finger improves control of ON-switch split CARs

The enhanced degradation enabled by super-degrons indicated more efficient zinc finger-lenalidomide-CRBN interactions. Increasing the drug-mediated interaction efficiency should improve ON-switch CAR performance. Therefore, we compared split CARs with dimerization domains engineered from IKZF3 or ZFP91-IKZF3 (split CAR_I and split CAR_H, respectively) (Fig. 4A). Both zinc finger-containing sequences included mutations of all intracellular Lys residues to Arg residues to prevent ubiquitination. When Jurkat T cells expressing these split CARs were exposed to CD19+ target cells and a range of lenalidomide concentrations, the EC50 to increase the percent of CD69-positive cells was 7-fold lower for split CAR_H compared to split CAR_I (Fig. 4B); therefore, we focused on split CAR_H in subsequent experiments.

Lenalidomide ON-switch control of split CAR T cell function

To evaluate whether effector functions of primary T cells could be controlled by lenalidomide, we transduced primary human T cells with vectors for split CAR_H. The split CAR components were delivered by two separate lentiviral vectors with different fluorescent protein markers. Thus, we used FACS to purify cells expressing neither, one, or both components (Fig. 4C). NALM6 B-ALL target cell killing was restricted to T cells expressing both components of the split CAR and exposed to 1 μM lenalidomide (Fig. 4D). Compared to a control second generation CAR, cytotoxicity of the split CAR was similar at high and moderate effector:target ratios but was lower than the control CAR once target cells exceeded the number of effector cells (Fig. 4E). When tested across a range of lenalidomide concentrations, the EC50 for cytotoxicity and interferon-gamma (IFN-γ) production induced by split CAR_H were 1 – 2 orders of magnitude below the 1.9 μM maximum plasma concentration of lenalidomide in multiple myeloma patients with 25 mg per day dosing (31) (Fig. 4F). Proliferation of split CAR T cells cultured with NALM6 target cells was dependent on lenalidomide (Fig. 4G). In summary, split CAR T cells demonstrated titratable T cell activation, tumor cell killing, proliferation, and cytokine release at clinically relevant lenalidomide concentrations, albeit at lower potency than the highly active conventional CAR control.

We evaluated lenalidomide ON-switch split CAR T cells in vivo for both anti-tumor potency and reversibility of drug regulation. Nonobese scid common gamma chain knockout (NSG) mice were engrafted with CD19+ luciferase+ JeKo-1 mantle cell lymphoma cells. Six days later, CAR or untransduced control T cells were injected, after which mice were left untreated or treated daily with 50 mg/kg pomalidomide for 11 consecutive days (Fig. 4H). Pomalidomide, which has similar activity and toxicity as lenalidomide and the same degron specificity (17, 18), was used for in vivo experiments because it has a longer in vivo half-life than lenalidomide. The control conventional CAR T cells mediated the most rapid and complete tumor depletion (Fig. 4I), consistent with their higher potency in vitro. With the split CAR_H, we observed a reduction in overall tumor burden (Fig. 4I–J) and enhanced expansion of the T cell population (Fig. 4K) during pomalidomide treatment. After cessation of pomalidomide treatment, residual tumor burden expanded, and the population of human T cells contracted in the peripheral blood. At the endpoint of the study, the percentage of human T cells in the spleen and bone marrow was comparable for the split CAR_H with or without pomalidomide (Fig. 4L). In summary, split CAR_H T cells demonstrated reversible lenalidomide ON-switch control of anti-tumor activity and T cell proliferation both in vitro and in vivo.

A super-degron improves control of OFF-switch degradable CARs

To test whether the super-degron also improved OFF-switch CAR control, we transduced Jurkat cells to express CD19-targeted CARs with either 4–1BB or CD28 costimulatory domains and lacking a degron (CAR) or containing the IKZF3 degron (ID-CAR), the ZFP91-IKZF3 super-degron (SD-CAR), or the super-degron with a Cys-to-Ala substitution at the zinc-chelating position in ZFP91 (mutSD-CAR), which confers drug insensitivity (fig. S5A). With either costimulatory domain and in response to either lenalidomide or pomalidomide, SD-CAR was more efficiently degraded than ID-CAR (fig. S5B, S5C, S5D).

Furthermore, these differences were reflected by differential effects on functional activity, measured as reduction of CD69+ cells and reduced secretion of interleukin-2 (IL-2). As expected, the cells expressing the mutSD-CAR were not affected by either thalidomide analog. Lenalidomide had greater efficacy in reducing the abundance of the CAR and the percent of CD69+ cells in cells expressing 4–1BB-based CARs than in cells expressing CD28-based CARs (compare fig. S5B and S5D). Therefore, we focused primarily on 4–1BB-based CARs.

We confirmed lenalidomide dose-dependent depletion of 4–1BB degradable CARs by Western blotting (Fig. 5B). Little of SD-CAR was detectable in cells exposed to 1 nM lenalidomide. In contrast, ID-CAR was readily detected at the same concentration. Degradation of the canonical endogenous substrate IKZF3 was evident with 100 nM lenalidomide. To confirm that degradation involved a Cullin-RING ligase-dependent mechanism (14, 15), we examined cells expressing SD-CAR for stabilizing effects of an E1 inhibitor (MLN7243), a neddylation inhibitor (MLN4294), and lysosomal acidification inhibitors (chloroquine or bafilomycin A). CAR degradation was inhibited by MLN7243 and MLN4294 (Fig. 5B) and was insensitive to chloroquine or bafilomycin A (fig. S6).

We also examined the kinetics of OFF-switch CAR depletion after the addition of lenalidomide. Half-maximal depletion of SD-CAR occurred in ~20 minutes (fig. S7A). We examined the dynamics of CAR re-synthesis after washout of lenalidomide. Half-maximal recovery of degradable CAR abundance occurred after ~3.6 hours (fig. S7B). In sum, we established that posttranslational control of degradable CAR protein abundance was rapid and reversible, consistent with the degradation kinetics of other thalidomide analog substrate proteins (17). These findings demonstrated reversible pharmacologic control of CAR abundance.

Lenalidomide controls degradable CAR T cell effector functions in vitro

We next evaluated whether effector functions of degradable CAR T cells could be controlled with lenalidomide. Primary human T cells were transduced to express conventional CAR or SD-CAR. Lenalidomide selectively mediated degradation of SD-CAR in both CD4+ and CD8+ cells (Fig. 5C). Conventional CAR abundance was insensitive to lenalidomide. In coculture assays in which NALM6 target cells and lenalidomide were pre-mixed and then simultaneously added to T cells, 100 nM lenalidomide completely inhibited target cell killing by SD-CAR T cells at all effector:target ratios tested (Fig. 5D). Complete inhibition of cytolysis indicated rapid kinetics of functional inhibition, consistent with the rapid kinetics of CAR depletion (fig. S7A). We then analyzed cytokine production in response to antigen stimulation. As expected, cells expressing conventional CAR increased production of IL-2 when cocultured with target cells in the presence of lenalidomide (Fig. 5E). Conversely, lenalidomide reduced the secretion of all evaluated cytokines from SD-CAR T cells cocultured with target cells, indicating reduced T cell activation. Inhibition of cytotoxicity and release of all evaluated cytokines indicated OFF-switch function in both CD8 and CD4 T cell subsets. When tested across a range of lenalidomide concentrations, half-maximal inhibition of cytotoxicity and cytokine production from SD-CAR T cells were observed at approximately 1/100 of the maximum plasma concentration of lenalidomide

with 25 mg per day dosing in patients (Fig. 5F). Proliferation of SD-CAR T cells stimulated with NALM6 target cells was inhibited by lenalidomide (Fig. 5G). In summary, addition of the super-degron enabled lenalidomide OFF-switch control of CAR T cell effector functions.

We evaluated cytolytic activity, cytokine secretion, and T cell proliferation for conventional CAR and SD-CAR T cells cocultured with low antigen NALM6 clones (fig. S8A). SD-CAR T cells retained similar cytolytic capacity as conventional CAR T cells in the setting of reduced antigen stimulation (fig. S8B). Only a modest reduction in cytokine release differentiated SD-CAR versus conventional CAR T cells (**fig. 8C**). CAR- or SD-CAR-expressing cells exhibited similar proliferation when cultured with either antigen-low ($CD19^{low}$) or parental wild-type target cells (**fig. 8D**). To test degradable CARs against an alternative target antigen, we generated SD-CARs targeting the antigen BCMA. We confirmed lenalidomide reduced the abundance of the BCMA-targeted SD-CAR (fig. S9A). When cocultured with BCMA+ RPMI 8226 myeloma cells, lenalidomide reduced anti-BCMA SD-CAR T cell cytotoxicity, cytokine production, and proliferation (fig. S9B, S9C, S9D). In summary, SD-CAR T cells were generalizable to multiple target antigens and target antigen densities.

CD28 costimulatory domain-specific effects on degradable CARs

CAR T cells using 4–1BB or CD28 costimulatory domains are clinically approved, and have well-characterized differences in signal transduction, effector functions, and persistence (32). CARs with CD28 costimulation enforce strong T cell activation, resulting in rapid anti-tumor effect but also T cell exhaustion and limited persistence (33). We generated SD-CAR constructs with CD28 transmembrane and intracellular domains, along with the CD3z signaling domain (fig. S10A). Surprisingly, in this context, the super-degron resulted in markedly reduced cell surface abundance of the SD-CAR in both CD4+ and CD8+ cells compared with the abundance of conventional CAR, even in the absence of lenalidomide (fig. S10B). Despite this low abundance, CD28 SD-CAR T cells exhibited cytotoxicity against NALM6 target cells, which was partially inhibited with 1000 nM lenalidomide (fig. S10C). In this co-culture assay, 1000 nM lenalidomide partially inhibited the release of multiple cytokines, including IL-13, granulocyte-macrophage colony-stimulating factor (GM-CSF), IFN-γ, and IL-18, from CD28 SD-CAR T cells (fig. S10D). Of note, without drug treatment, cytokine release was on average higher from the conventional versus the SD-CAR T cells (data file S1).

Although the CD28 SD-CAR was relatively hypofunctional in vitro, in vivo control of Jeko-1 lymphoma cells in mice was greater than that of conventional CAR T cells, when evaluated either as tumor bioluminescence (fig. S10E, S10F) or as tumor cell burden in harvested spleen (fig. S10G). Furthermore, T cell persistence in the bone marrow was higher for CD28 SD-CAR T cells versus those with conventional CAR (fig. S10H). In summary, these findings showed that the super-degron reduced the abundance of a CAR with the CD28 costimulatory domain, yet these degradable CARs demonstrated lenalidomide OFF-switch regulation and retained anti-tumor activity in vivo.

CAR degradation is reversible in vivo

We next evaluated the kinetics of degradable CAR depletion in vivo. We generated CAR-luciferase fusions tagged with either the super-degron or, as a negative control, mutated super-degron to monitor CAR abundance with bioluminescent imaging (Fig. 6A). As expected, after exposure to lenalidomide, we observed a dose-dependent decrease in luminescence from Jurkat cells expressing degradable but not control luciferase-tagged CARs (fig. S11). Target antigen stimulation is required for primary human CAR T cell engraftment in immunocompromised mouse models, but antigen-dependent CAR signaling results in endocytosis of the receptor and would confound measurement of drug-dependent CAR degradation. To overcome this issue, we measured in vivo pomalidomide-induced degradation of SD-CARs by engrafting NSG mice with Jurkat T cells transduced with luciferase-tagged CARs. The engraftment, proliferation, and receptor kinetics of these cells are independent from the cognate antigen of the CAR. After establishing detectable engraftment of Jurkat cells expressing luciferase-tagged CARs by bioluminescent imaging, we administered a single 10 mg/kg pomalidomide dose by oral gavage (Fig. 6B). Six hours after drug treatment, luminescence from SD-CAR was reduced by 5-fold compared to that of the mutSD-CAR (Fig. 6C,D). After 24 hours, luminescence had recovered to amounts similar to that prior to drug administration and both mutSD-CAR and SD-CAR abundance was similar (Fig. 6C, D). Thus, the in vivo kinetics of degradation and re-appearance of SD-CARs were consistent with our in vitro findings, and suggested that daily dosing of lenalidomide or pomalidomide would transiently abrogate CAR expression, with recovery of CAR abundance upon drug discontinuation.

Super-degron degradable CAR T cells exhibit anti-tumor activity

Subtle sequence changes to CARs have been associated with intended and unintended consequences for CAR T cell efficacy and toxicity in clinical trials, as well as in pre-clinical models (34–36). Therefore, we determined whether addition of the zinc finger super-degron impacts CAR T cell activity in a mantle cell lymphoma xenograft model. We engrafted NSG mice with CD19+ luciferase+ JeKo-1 mantle cell lymphoma cells. One week later, we injected 4–1BB-based CAR, SD-CAR, or untransduced control T cells (Fig. 7A). Tumor burden was followed by bioluminescent imaging (Fig. 7B). Tumor burden and T cell persistence were comparable between animals receiving cells with SD-CARs or conventional CARs (Fig. 7C, D, E). Thus, in this setting the super-degron appeared a neutral change for in vivo CAR T cell function.

Pomalidomide suppresses cytokine release from super-degron degradable CAR T cells

We evaluated whether degradable CAR T cell cytokine release was controlled with pomalidomide in vivo, ideally at a drug concentration that spares anti-tumor effect. Having identified a pomalidomide treatment dose and schedule that did not significantly alter anti-tumor activity (fig. S12A–E), we then used this regimen in a high-level tumor engraftment model that provoked robust CAR T cell cytokine release. NALM6 cells were engrafted in NSG mice one week before injection of SD-CAR or untransduced control T cells. On days 3 – 5 after T cell transfer, mice were either left untreated, treated daily, or treated twice daily with 30 mg/kg pomalidomide (Fig. 7F). On the afternoon of day 5, serum concentrations

were measured for a panel of human T cell cytokines. Compared with amounts in untreated mice, IFN-γ concentrations were reduced four-fold with daily and six-fold with twice-daily pomalidomide treatment (Fig. 7G). IL-2 concentrations were reduced four-fold with daily treatment (Fig. 7H. Thus, pomalidomide limited cytokine release, the major driver of CAR T cell hyperactivation toxicities.

Discussion

Here, we established chemical genetic control of CAR T cells using human sequences and a clinically approved, non-immunosuppressive small molecule controller. Regulated transgene function has the potential to improve diverse gene- and cell-based therapies. User control of therapeutics could enable use of highly active therapeutic proteins that would be toxic if constitutively present (37). Although many synthetic gene regulation tools have been developed (38), most use non-human components, small molecule controllers that have not been clinically validated or immunosuppressive drugs, such as rapamycin, that may limit CAR T cell efficacy.

The ternary complex interactions between ubiquitin ligases, targeted protein degraders, and polypeptide degrons are a rich starting point to engineer synthetic control modules. For clinical use, engineering efficient molecular switches regulated by subtherapeutic lenalidomide doses is important to minimize the risk of drug side effects, including myelosuppression (39). We performed a systematic screen to engineer super-degrons that are depleted in the presence of low concentrations of lenalidomide. Whereas previous efforts engineered the DNA sequence specificity of zinc fingers by altering DNA-contacting residues (40), here we leveraged the modularity of beta-hairpin and alpha-helix subdomains to build a library of hybrid zinc fingers. We were surprised that almost 5% of the hybrid zinc fingers were more efficiently degraded than the parent zinc finger degrons that had previously been discovered through screens of all C2H2 zinc fingers in the proteome for thalidomide analog-induced degradation (18). Scalable functional genomic and directed evolution approaches may uncover the sequence and structural determinants for enhanced CRBN-drug interactions, as well as even higher affinity, bio-orthogonal super-degrons that can be depleted at lenalidomide doses that spare endogenous substrates. Already, SD-CAR was depleted at ~ 100-fold lower lenalidomide concentrations than those required to deplete endogenous IKZF3.

As a proof of concept, we tested our chemical genetic switches in CARs to address a clinical need and the challenge of regulating sensitive and highly active receptors that require near-complete control for robust switch-regulatable function. We engineered a lenalidomide-inducible dimerization system, which we used to gate two-component split CARs. These ON-switch split CARs demonstrated tunable anti-tumor activity in vitro and in vivo. We also developed lenalidomide-OFF-switch degradable CARs, which demonstrated control of T cell effector functions at or below therapeutic drug doses. The particular robustness of the degradable CAR may be due to “substoichiometric” pharmacologic effects of targeted protein degraders, wherein a single molecule can induce the degradation of many target proteins through serial docking interactions with $CRL4^{CRBN}$ and substrate proteins (41). In vivo, cells with degradable and conventional CARs exhibited similar anti-tumor activity and

T cell persistence. A single dose of pomalidomide induced time-limited CAR degradation, and a short course of pomalidomide inhibited inflammatory cytokine release.

With respect to limitations, lenalidomide ON-switch split CAR T cells were slightly less active than conventional CAR T cells. Controllable, less potent CAR T cells may prove to be safe at higher cell doses and could be tested against target antigens associated with safety concerns. The addition of a degron had variable effects on CAR abundance. In our experience, all evaluated degradable CAR constructs were active and controllable with lenalidomide. In future applications, if necessary, effects of degron or dimerization domains on receptor function could be mitigated by altering gene dosage or per-molecule signaling strength along established lines (34, 36, 42, 43).

Numerous approaches to mitigate CAR T cell toxicities have been proposed (38). Rapalog-based pharmacologic ON switches have achieved graded activation and temporal control (29). Protein-based ON switches enable flexible antigen targeting from a single cellular product (44). A suicide switch, such as a small molecule-inducible caspase system (45), can terminate a CAR T cell response. Dasatinib inhibits proximal signaling downstream of the T cell receptor (46, 47) and CAR (48, 49). Importantly, dasatinib can reversibly control CAR T cell effector functions and alleviate cytokine production in models of cytokine release syndrome (48, 49), demonstrating the potential therapeutic value of proximal CAR signal inhibition. Whereas only nonspecific therapies like corticosteroids or dasatinib can regulate the currently marketed CAR T cells, lenalidomide-gated chemical genetic switches offer the unique benefits of (i) specific CAR inhibition that spares normal T cell receptor signaling and (ii) generalizability to regulate diverse transgenes. Many of these approaches may prove complementary.

In the near-term, one critical aspect of the development of drug-regulated CARs will be defining the clinical and biomarker parameters that clinicians should use to decide when to turn the CAR on or off. Initially, development of OFF-switch CARs could be tested in well-defined entities such as cytokine release syndrome, for which the typical time course is days to weeks soon after CAR T cell infusion. In contrast, ON-switch CARs may be of greatest initial use in advancing novel targets that have not been fully validated in the clinic, and may have low-level abundance in normal tissues, including CARs for most solid tumors. In this case, cessation of the drug would liberate the patient from long-term use of both the drug and the CAR activity.

Beyond mitigating toxicity, lenalidomide-gated CARs enable novel therapeutic opportunities. Using dasatinib or a destabilization domain, transient rest from CAR signaling protects against T cell exhaustion (50); future work may establish whether lenalidomide ON- or OFF-switch control enhances the phenotype and function of exhaustion-prone CARs. Future work will also determine the effect of lenalidomide-based control on CAR T cells after prolonged exposure to various disease-specific tumor microenvironments. Third generation CARs, switch receptors (51, 52), armored CARs (53), and other approaches to enhance T cell effector functions and persistence could be controlled by dimerization or degradation. The potent immunomodulatory and anti-tumor effects of lenalidomide may be useful in some situations. Already, lenalidomide enhances the function of second-generation

CAR T cells targeting multiple myeloma and glioblastoma multiforme (54–56). For lenalidomide- or pomalidomide-sensitive malignancies, the CAR and the controller drug could together mediate dual orthogonal mechanisms of tumor targeting. Together, our split and degradable CAR T cells may combine favorable effects on T cell signaling, phenotype, and tumor targeting.

Materials and Methods

Study design

The objective of the study was to engineer lenalidomide-induced degradation and dimerization molecular switches using pooled, sequencing-based assays for protein degradation as well as bioluminescence resonance energy transfer assays for protein dimerization. These molecular switches were then used to design lenalidomide ON- and OFF-switch CARs incorporating multiple tumor-targeting and signaling domains. Switch-regulated CARs were functionally evaluated in Jurkat and primary human T cell models using assays for T cell activation, cytotoxicity, cytokine release, and proliferation. In mouse models, tumor growth was measured by bioluminescence, human T cells were enumerated in the blood, bone marrow, and spleen, and human cytokine abundance was measured in plasma samples. Cell line experiment replicates were variable and are indicated in the figure legends. In vitro and in vivo primary cell experiments were performed multiple times with T cells derived from a variety of normal human donors, with the exception of the in vivo SD-CAR cytokine release model, which was performed once with multiple drug conditions in parallel. For in vivo experiments, mice were randomly assigned to groups on the basis of tumor burden. The study was not blinded.

C2H2 zinc finger hybrid degron library screen

Jurkat cells expressing a library of 440 C2H2 zinc fingers in an eGFP/mCherry protein degradation reporter vector were treated with DMSO or a thalidomide analog for 16 hours. $mCherry^{+}eGFP^{low}$ cell populations were isolated by FACS in triplicate, and the relative abundance of individual zinc fingers was quantified with next-generation sequencing. The relative abundance of each zinc finger was then ranked, summed, and compared to a simulated normal distribution. For validation, Jurkat cells were engineered to express individual zinc fingers in the protein degradation reporter; the eGFP:mCherry ratio was determined by flow cytometry after 16 hour incubation with varying concentrations of thalidomide analogs.

Construction of chimeric antigen receptors

Transgenes were synthesized and cloned into lentiviral vectors. Split CAR component A was constructed using the CSF2RA signal sequence, Myc tag, anti-CD19 scFv (FMC63), and the CD28 hinge, transmembrane, and co-stimulatory domains, along with the zinc finger dimerization domain, a P2A element, and mCherry. Split CAR component B was constructed using the CD8 alpha signal sequence, hinge, and transmembrane domains, CD28 costimulatory domain, CRBNΔ3, CD3z intracellular domain, and eGFP. A number of degradable CAR constructs were generated, encoding the CD8 alpha signal sequence, Myc tag, scFv targeting CD19 or BCMA, hinge domain from IgG4 or CD8 alpha, transmembrane

domain from CD28 or CD8 alpha, co-stimulatory domain from CD28 or 4–1BB, and CD3z domain. Transduced cells were detected by eGFP or mCherry expression.

NanoBRET proximity-based assays

Transgenes were synthesized and cloned into plasmids in frame with NanoLuc or HaloTag (Promega). Plasmids were co-transfected into 293T cells, and 24 hours later cells were treated with pomalidomide or vehicle control, as well as MG132 (10 μM) in some experiments. 2 hours thereafter, the HaloTag 618 ligand was added and both NanoLuc and HaloTag ligand emission was measured with an EnVision plate reader (PerkinElmer). mBU (miliBRET units) = HaloTag ligand emission / Nanoluc emission x 1,000.

Jurkat CAR protein degradation and functional assays

Jurkat cells transduced with lentiviral vectors encoding CARs were cocultured for 16 hours with either K562 target cells or K562 cells engineered to express CD19 in a 5:1 ratio. Jurkat CAR T cells were then assessed by flow cytometry for CAR (anti-Myc tag; Cell Signaling Technology, 2233) and CD69 abundance (Biolegend, 310920). Normalized CAR abundance was calculated by subtraction of the mean fluorescence intensity of unstained cells and normalization to the signal intensity of vehicle control-treated cells. IL-2 concentration in the coculture supernatant was assessed by IL-2 ELISA (BD Biosciences, 555190). Luciferase-tagged CAR luminescence was measured with an EnVision plate reader (PerkinElmer).

T cell culture transduction

Human T cells were purified (Stem Cell Technologies, 15061) from anonymous human healthy donor leukopacs obtained from the Massachusetts General Hospital blood bank under an Institutional Review Board-approved protocol. Primary T cell stimulation, transduction, and expansion was performed as previously described (57).

Cellular cytotoxicity, cytokine, and proliferation assays

Primary human CAR T effector cells were cocultured with target cells engineered to express click beetle green luciferase. Cells were cocultured at the indicated ratios for 16 hours. Luciferase activity was measured with a Synergy Neo2 luminescence microplate reader (Biotek). Cell culture supernatant from these experiments was analyzed for soluble cytokines (Luminex or BD Biosciences Cytometric Bead Array). Primary human CAR T effector cells were covalently labeled with CellTrace Violet (ThermoFisher), cocultured with target cells for 3 – 5 days, and analyzed by flow cytometry.

In vivo studies

All animal procedures were performed in accordance with Federal and Institutional Animal Care and Use Committee requirements under protocols approved at the Broad Institute or Massachusetts General Hospital. Mice were treated with the indicated pomalidomide dose. Pomalidomide was solubilized in DMSO, and then diluted in PBS immediately prior to treatment. Bioluminescence imaging was performed using an IVIS Spectrum in vivo

imaging system. Serum cytokine assays were performed per manufacturer's instructions (Luminex or BD Cytometric Bead Array).

Statistical analysis

Data are presented as means ± SD. The alpha level was 0.05. Statistical analyses were performed in GraphPad Prism, using two-tailed Student's *t* tests or two-way analysis of variance (ANOVA) as indicated. The Tukey method was used to correct for multiple comparisons.

Supplementary Material

Refer to Web version on PubMed Central for supplementary material.

Acknowledgements

The authors thank members of the Maus and Ebert labs for feedback and discussion, in particular R. Belizaire, D. Levin, and T. Berger for comments on the manuscript. Editorial services were provided by Nancy R. Gough (BioSerendipity, LLC, Elkridge, MD). Icons from Biorender.com.

Funding

MJ is supported by a NIH T32 grant to the Massachusetts General Hospital Department of Pathology (NIH-5T32CA009216-39). MVM is supported by grants from Gabrielle's Angel Foundation, the V Foundation, Stand up to Cancer, and the Damon Runyon Foundation. This work was supported by the NIH (R01HL082945, P01CA108631, and P50CA206963), the Howard Hughes Medical Institute, the Edward P. Evans Foundation, and the Leukemia and Lymphoma Society to BLE.

Competing Interests

MJ, MVM, and BLE are inventors on patent application W02019089592 held by the Broad Institute that covers lenalidomide switch control of engineered cells. MJ and BLE are inventors on patent application U.S. Provisional Application No. 62/983,448 held by the Broad Institute that covers zinc finger degradation domains. MVM has received consulting income from Adaptimmune, Allogene, Arcellx, CRISPR Therapeutics, GSK, Incysus, KitePharma, Novartis, TCR2, and WindMIL, has equity in Century Therapeutics and TCR2, and she receives sponsored research support from CRISPR therapeutics and KitePharma; none of the above is related to this work. BLE has received research funding from Celgene and Deerfield. He has received consulting fees from GRAIL, and he serves on the scientific advisory boards for and holds equity in Skyhawk Therapeutics and Exo Therapeutics.

Data and materials availability

All data associated with this study are provided in the manuscript or the Supplementary Materials.

References and notes

1. Fischbach MA, Bluestone JA, Lim WA, Cell-Based Therapeutics: The Next Pillar of Medicine, Sci Transl Med 5, 179ps7–179ps7 (2013).
2. Sadelain M, Rivière I, Riddell S, Therapeutic T cell engineering, Nature 545, 423–431 (2017). [PubMed: 28541315]
3. Milone MC, Bhoj VG, The Pharmacology of T Cell Therapies, Mol Ther - Methods Clin Dev 8, 210–221 (2018). [PubMed: 29552577]
4. Neelapu SS, Tummala S, Kebriaei P, Wierda W, Gutierrez C, Locke FL, Komanduri KV, Lin Y, Jain N, Daver N, Westin J, Gulbis AM, Loghin ME, de Groot JF, Adkins S, Davis SE, Rezvani K, Hwu P, Shpall EJ, Chimeric antigen receptor T-cell therapy - assessment and management of toxicities., Nat Rev Clin Oncol 15, 47–62 (2017). [PubMed: 28925994]

5. Bedoya F, Frigault MJ, Maus MV, The Flipside of the Power of Engineered T Cells: Observed and Potential Toxicities of Genetically Modified T Cells as Therapy, Mol Ther 25, 314–320 (2017). [PubMed: 28153085]
6. Davila ML, Riviere I, Wang X, Bartido S, Park J, Curran K, Chung SS, Stefanski J, Borquez-Ojeda O, Olszewska M, Qu J, Wasielewska T, He Q, Fink M, Shinglot H, Youssif M, Satter M, Wang Y, Hosey J, Quintanilla H, Halton E, Bernal Y, Bouhassira DCG, Arcila ME, Gonen M, Roboz GJ, Maslak P, Douer D, Frattini MG, Giralt S, Sadelain M, Brentjens R, Efficacy and toxicity management of 19–28z CAR T cell therapy in B cell acute lymphoblastic leukemia., Sci Transl Med 6, 224ra25 (2014).
7. Frey NV, Shaw PA, Hexner EO, Pequignot E, Gill S, Luger SM, Mangan JK, Loren AW, Perl AE, Maude SL, Grupp SA, Shah NN, Gilmore J, Lacey SF, Melenhorst JJ, Levine BL, June CH, Porter DL, Optimizing Chimeric Antigen Receptor T-Cell Therapy for Adults With Acute Lymphoblastic Leukemia, J Clin Oncol 38, 415–422 (2020). [PubMed: 31815579]
8. Raina K, Crews CM, Chemical inducers of targeted protein degradation., J Biological Chem 285, 11057–60 (2010).
9. Banaszynski LA, Chen L, Maynard-Smith LA, Ooi AGL, Wandless TJ, A Rapid, Reversible, and Tunable Method to Regulate Protein Function in Living Cells Using Synthetic Small Molecules, Cell 126, 995–1004 (2006). [PubMed: 16959577]
10. Nishimura K, Fukagawa T, Takisawa H, Kakimoto T, Kanemaki M, An auxin-based degron system for the rapid depletion of proteins in nonplant cells, Nat Methods 6, 917–922 (2009). [PubMed: 19915560]
11. Bonger KM, Chen L, Liu CW, Wandless TJ, Small-molecule displacement of a cryptic degron causes conditional protein degradation, Nat Chem Biol 7, 531–537 (2011). [PubMed: 21725303]
12. Chung HK, Jacobs CL, Huo Y, Yang J, Krumm SA, Plemper RK, Tsien RY, Lin MZ, Tunable and reversible drug control of protein production via a self-excising degron, Nat Chem Biol 11, 713–720 (2015). [PubMed: 26214256]
13. Nabet B, Roberts JM, Buckley DL, Paulk J, Dastjerdi S, Yang A, Leggett AL, Erb MA, Lawlor MA, Souza A, Scott TG, Vittori S, Perry JA, Qi J, Winter GE, Wong K-K, Gray NS, Bradner JE, The dTAG system for immediate and target-specific protein degradation, Nat Chem Biol 14, 431–441 (2018). [PubMed: 29581585]
14. Krönke J, Udeshi ND, Narla A, Grauman P, Hurst SN, McConkey M, Svinkina T, Heckl D, Comer E, Li X, Ciarlo C, Hartman E, Munshi N, Schenone M, Schreiber SL, Carr SA, Ebert BL, Lenalidomide causes selective degradation of IKZF1 and IKZF3 in multiple myeloma cells., Sci New York N Y 343, 301–5 (2013).
15. Lu G, Middleton RE, Sun H, Naniong M, Ott CJ, Mitsiades CS, Wong K-K, Bradner JE, Kaelin WG, The myeloma drug lenalidomide promotes the cereblon-dependent destruction of Ikaros proteins., Sci New York N Y 343, 305–9 (2013).
16. Krönke J, Fink EC, Hollenbach PW, MacBeth KJ, Hurst SN, Udeshi ND, Chamberlain PP, Mani DR, Man HW, Gandhi AK, Svinkina T, Schneider RK, McConkey M, Järås M, Griffiths E, Wetzler M, Bullinger L, Cathers BE, Carr SA, Chopra R, Ebert BL, Lenalidomide induces ubiquitination and degradation of CK1α in del(5q) MDS, Nature 523, 183–188 (2015). [PubMed: 26131937]
17. Sperling AS, Burgess M, Keshishian H, Gasser JA, Bhatt S, Jan M, Słabicki M, Sellar RS, Fink EC, Miller PG, Liddicoat BJ, Sievers QL, Sharma R, Adams DN, Olesinski EA, Fulciniti M, Udeshi ND, Kuhn E, Letai A, Munshi NC, Carr SA, Ebert BL, Patterns of substrate affinity, competition, and degradation kinetics underlie biological activity of thalidomide analogs., Blood 134, 160–170 (2019). [PubMed: 31043423]
18. Sievers QL, Petzold G, Bunker RD, Renneville A, Słabicki M, Liddicoat BJ, Abdulrahman W, Mikkelsen T, Ebert BL, Thomä NH, Defining the human C2H2 zinc finger degrome targeted by thalidomide analogs through CRBN, Science 362, eaat0572 (2018). [PubMed: 30385546]
19. An J, Ponthier CM, Sack R, Seebacher J, Stadler MB, Donovan KA, Fischer ES, pSILAC mass spectrometry reveals ZFP91 as IMiD-dependent substrate of the CRL4CRBN ubiquitin ligase, Nat Commun 8, 15398 (2017). [PubMed: 28530236]

20. Donovan KA, An J, Nowak RP, Yuan JC, Fink EC, Berry BC, Ebert BL, Fischer ES, Thalidomide promotes degradation of SALL4, a transcription factor implicated in Duane Radial Ray syndrome, Elife 7, e38430 (2018). [PubMed: 30067223]
21. Matyskiela ME, Couto S, Zheng X, Lu G, Hui J, Stamp K, Drew C, Ren Y, Wang M, Carpenter A, Lee C-W, Clayton T, Fang W, Lu C-C, Riley M, Abdubek P, Blease K, Hartke J, Kumar G, Vessey R, Rolfe M, Hamann LG, Chamberlain PP, SALL4 mediates teratogenicity as a thalidomide-dependent cereblon substrate, Nat Chem Biol 14, 981–987 (2018). [PubMed: 30190590]
22. June CH, Sadelain M, Chimeric Antigen Receptor Therapy, New Engl J Med 379, 64–73 (2018). [PubMed: 29972754]
23. Hay KA, Hanafi L-A, Li D, Gust J, Liles WC, Wurfel MM, López JA, Chen J, Chung D, Harju-Baker S, Cherian S, Chen X, Riddell SR, Maloney DG, Turtle CJ, Kinetics and biomarkers of severe cytokine release syndrome after CD19 chimeric antigen receptor–modified T-cell therapy, Blood 130, 2295–2306 (2017). [PubMed: 28924019]
24. Fink EC, Ebert BL, The novel mechanism of lenalidomide activity., Blood 126, 2366–9 (2015). [PubMed: 26438514]
25. Hamann J, Fiebig H, Strauss M, Expression cloning of the early activation antigen CD69, a type II integral membrane protein with a C-type lectin domain., J Immunol Baltim Md 1950 150, 4920–7 (1993).
26. Fischer ES, Böhm K, Lydeard JR, Yang H, Stadler MB, Cavadini S, Nagel J, Serluca F, Acker V, Lingaraju GM, Tichkule RB, Schebesta M, Forrester WC, Schirle M, Hassiepen U, Ottl J, Hild M, Beckwith REJ, Harper JW, Jenkins JL, Thomä NH, Structure of the DDB1–CRBN E3 ubiquitin ligase in complex with thalidomide, Nature 512, 49–53 (2014). [PubMed: 25043012]
27. Petzold G, Fischer ES, Thomä NH, Structural basis of lenalidomide-induced CK1α degradation by the CRL4CRBN ubiquitin ligase, Nature 532, 127–130 (2016). [PubMed: 26909574]
28. Chamberlain PP, Lopez-Girona A, Miller K, Carmel G, Pagarigan B, Chie-Leon B, Rychak E, Corral LG, Ren YJ, Wang M, Riley M, Delker SL, Ito T, Ando H, Mori T, Hirano Y, Handa H, Hakoshima T, Daniel TO, Cathers BE, Structure of the human Cereblon–DDB1–lenalidomide complex reveals basis for responsiveness to thalidomide analogs, Nat Struct Mol Biol 21, 803–809 (2014). [PubMed: 25108355]
29. Wu C-Y, Roybal KT, Puchner EM, Onuffer J, Lim WA, Remote control of therapeutic T cells through a small molecule-gated chimeric receptor, Science 350, aab4077–aab4077 (2015). [PubMed: 26405231]
30. Leung W-H, Gay J, Martin U, Garrett TE, Horton HM, Certo MT, Blazar BR, Morgan RA, Gregory PD, Jarjour J, Astrakhan A, Sensitive and adaptable pharmacological control of CAR T cells through extracellular receptor dimerization, Jci Insight 4 (2019), doi:10.1172/jci.insight.124430.
31. Chen N, Zhou S, Palmisano M, Clinical Pharmacokinetics and Pharmacodynamics of Lenalidomide, Clin Pharmacokinet 56, 139–152 (2017). [PubMed: 27351179]
32. Weber EW, Maus MV, Mackall CL, The Emerging Landscape of Immune Cell Therapies, Cell 181, 46–62 (2020). [PubMed: 32243795]
33. Long AH, Haso WM, Shern JF, Wanhainen KM, Murgai M, Ingaramo M, Smith JP, Walker AJ, Kohler ME, Venkateshwara VR, Kaplan RN, Patterson GH, Fry TJ, Orentas RJ, Mackall CL, 4–1BB costimulation ameliorates T cell exhaustion induced by tonic signaling of chimeric antigen receptors, Nat Med 21, 581–590 (2015). [PubMed: 25939063]
34. Feucht J, Sun J, Eyquem J, Ho Y-J, Zhao Z, Leibold J, Dobrin A, Cabriolu A, Hamieh M, Sadelain M, Calibration of CAR activation potential directs alternative T cell fates and therapeutic potency, Nat Med 25, 82–88 (2018). [PubMed: 30559421]
35. Hudecek M, Sommermeyer D, Kosasih PL, Silva-Benedict A, Liu L, Rader C, Jensen MC, Riddell SR, The nonsignaling extracellular spacer domain of chimeric antigen receptors is decisive for in vivo antitumor activity., Cancer Immunol Res 3, 125–35 (2014). [PubMed: 25212991]
36. Ying Z, Huang XF, Xiang X, Liu Y, Kang X, Song Y, Guo X, Liu H, Ding N, Zhang T, Duan P, Lin Y, Zheng W, Wang X, Lin N, Tu M, Xie Y, Zhang C, Liu W, Deng L, Gao S, Ping L, Wang X, Zhou N, Zhang J, Wang Y, Lin S, Mamuti M, Yu X, Fang L, Wang S, Song H, Wang G, Jones L,

Zhu J, Chen S-Y, A safe and potent anti-CD19 CAR T cell therapy, Nat Med 25, 947–953 (2019). [PubMed: 31011207]

37. Chiocca EA, Yu JS, Lukas RV, Solomon IH, Ligon KL, Nakashima H, Triggs DA, Reardon DA, Wen P, Stopa BM, Naik A, Rudnick J, Hu JL, Kumthekar P, Yamini B, Buck JY, Demars N, Barrett JA, Gelb AB, Zhou J, Lebel F, Cooper LJN, Regulatable interleukin-12 gene therapy in patients with recurrent high-grade glioma: Results of a phase 1 trial, Sci Transl Med 11, eaaw5680 (2019). [PubMed: 31413142]
38. Brenner MJ, Cho JH, Wong NML, Wong WW, Synthetic Biology: Immunotherapy by Design, Annu Rev Biomed Eng 20, 95–118 (2018). [PubMed: 29345976]
39. Richardson PG, Schlossman RL, Weller E, Hideshima T, Mitsiades C, Davies F, LeBlanc R, Catley LP, Doss D, Kelly K, McKenney M, Mechlowicz J, Freeman A, Deocampo R, Rich R, Ryoo JJ, Chauhan D, Balinski K, Zeldis J, Anderson KC, Immunomodulatory drug CC-5013 overcomes drug resistance and is well tolerated in patients with relapsed multiple myeloma, Blood 100, 3063–3067 (2002). [PubMed: 12384400]
40. Pabo CO, Peisach E, Grant RA, Design and Selection of Novel Cys 2 His 2 Zinc Finger Proteins, Annu Rev Biochem 70, 313–340 (2001). [PubMed: 11395410]
41. Lai AC, Crews CM, Induced protein degradation: an emerging drug discovery paradigm., Nat Rev Drug Discov 16, 101–114 (2016). [PubMed: 27885283]
42. Eyquem J, Mansilla-Soto J, Giavridis T, van der Stegen SJC, Hamieh M, Cunanan KM, Odak A, Gönen M, Sadelain M, Targeting a CAR to the TRAC locus with CRISPR/Cas9 enhances tumour rejection, Nature 543, 113–117 (2017). [PubMed: 28225754]
43. Majzner RG, Rietberg SP, Sotillo E, Dong R, Vachharajani VT, Labanieh L, Myklebust JH, Kadapakkam M, Weber EW, Tousley AM, Richards RM, Heitzeneder S, Nguyen SM, Wiebking V, Theruvath J, Lynn RC, Xu P, Dunn AR, Vale RD, Mackall CL, Tuning the Antigen Density Requirement for CAR T Cell Activity., Cancer Discov, CD-19–0945 (2020).
44. Cho JH, Collins JJ, Wong WW, Universal Chimeric Antigen Receptors for Multiplexed and Logical Control of T Cell Responses, Cell 173, 1426–1438.e11 (2018). [PubMed: 29706540]
45. Diaconu I, Ballard B, Zhang M, Chen Y, West J, Dotti G, Savoldo B, Inducible Caspase-9 Selectively Modulates the Toxicities of CD19-Specific Chimeric Antigen Receptor-Modified T Cells, Mol Ther 25, 580–592 (2017). [PubMed: 28187946]
46. Schade AE, Schieven GL, Townsend R, Jankowska AM, Susulic V, Zhang R, Szpurka H, Maciejewski JP, Dasatinib, a small-molecule protein tyrosine kinase inhibitor, inhibits T-cell activation and proliferation, Blood 111, 1366–1377 (2008). [PubMed: 17962511]
47. Weichsel R, Dix C, Wooldridge L, Clement M, Fenton-May A, Sewell AK, Zezula J, Greiner E, Gostick E, Price DA, Einsele H, Seggewiss R, Profound inhibition of antigen-specific T-cell effector functions by dasatinib., Clin Cancer Res Official J Am Assoc Cancer Res 14, 2484–91 (2008).
48. Weber EW, Lynn RC, Sotillo E, Lattin J, Xu P, Mackall CL, Pharmacologic control of CAR-T cell function using dasatinib, Blood Adv 3, 711–717 (2019). [PubMed: 30814055]
49. Mestermann K, Giavridis T, Weber J, Rydzek J, Frenz S, Nerreter T, Mades A, Sadelain M, Einsele H, Hudecek M, The tyrosine kinase inhibitor dasatinib acts as a pharmacologic on/off switch for CAR T cells, Sci Transl Med 11, eaau5907 (2019). [PubMed: 31270272]
50. Weber EW, Lynn RC, Parker KR, Anbunathan H, Lattin J, Sotillo E, Good Z, Malipatlolla M, Xu P, Vandris P, Majzner RG, Qi Y, Chen L-C, Gentles AJ, Wandless TJ, Satpathy AT, Chang HY, Mackall CL, Transient “rest” induces functional reinvigoration and epigenetic remodeling in exhausted CAR-T cells, Biorxiv, 2020.01.26.920496 (2020).
51. Prosser ME, Brown CE, Shami AF, Forman SJ, Jensen MC, Tumor PD-L1 co-stimulates primary human CD8+ cytotoxic T cells modified to express a PD1:CD28 chimeric receptor, Mol Immunol 51, 263–272 (2012). [PubMed: 22503210]
52. Liu X, Ranganathan R, Jiang S, Fang C, Sun J, Kim S, Newick K, Lo A, June CH, Zhao Y, Moon EK, A Chimeric Switch-Receptor Targeting PD1 Augments the Efficacy of Second-Generation CAR T Cells in Advanced Solid Tumors, Cancer Res 76, 1578–1590 (2016). [PubMed: 26979791]
53. Yeku OO, Brentjens RJ, Armored CAR T-cells: utilizing cytokines and pro-inflammatory ligands to enhance CAR T-cell anti-tumour efficacy, Biochem Soc T 44, 412–418 (2016).

54. Works M, Soni N, Hauskins C, Sierra C, Baturevych A, Jones JC, Curtis W, Carlson P, Johnstone TG, Kugler D, Hause RJ, Jiang Y, Wimberly L, Clouser CR, Jessup HK, Sather B, Salmon RA, Ports MO, Anti–B-cell Maturation Antigen Chimeric Antigen Receptor T cell Function against Multiple Myeloma Is Enhanced in the Presence of Lenalidomide, Mol Cancer Ther 18, 2246–2257 (2019). [PubMed: 31395689]

55. Kuramitsu S, Ohno M, Ohka F, Shiina S, Yamamichi A, Kato A, Tanahashi K, Motomura K, Kondo G, Kurimoto M, Senga T, Wakabayashi T, Natsume A, Lenalidomide enhances the function of chimeric antigen receptor T cells against the epidermal growth factor receptor variant III by enhancing immune synapses, Cancer Gene Ther 22, 487–495 (2015). [PubMed: 26450624]

56. Wang X, Walter M, Urak R, Weng L, Huynh C, Lim L, Wong CW, Chang W-C, Thomas SH, Sanchez J, Yang L, Brown CE, Pichiorri F, Htut M, Krishnan AY, Forman SJ, Lenalidomide enhances the function of CS1 chimeric antigen receptor redirected T cells against multiple myeloma, Clin Cancer Res 24, clincanres.0344.2017 (2017).

57. Scarfò I, Ormhøj M, Frigault MJ, Castano AP, Lorrey S, Bouffard AA, van Scoyk A, Rodig SJ, Shay AJ, Aster JC, Preffer FI, Weinstock DM, Maus MV, Anti-CD37 chimeric antigen receptor T cells are active against B- and T-cell lymphomas., Blood 132, 1495–1506 (2018). [PubMed: 30089630]

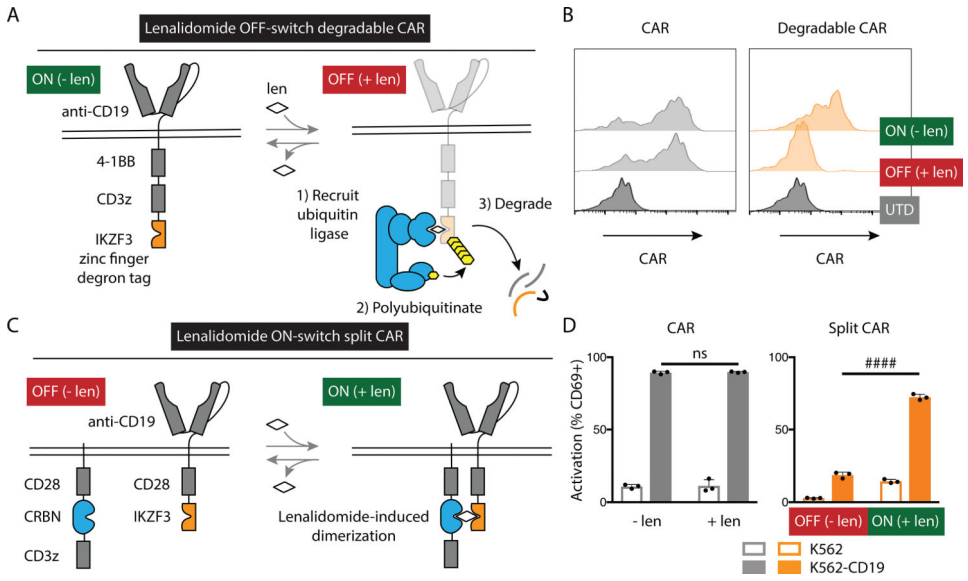

Fig. 1: Engineering lenalidomide ON- and OFF-switch controllable CAR T cells.

(A) Schematic of the OFF-switch degradable CARs and their degradation induced by lenalidomide (len) or other thalidomide analogs. The double line represents the plasma membrane with extracellular above the line and intracellular below the line. **(B)** Characterization of surface CAR abundance by flow cytometry using an antibody against the Myc tag (not shown in the schematic). Jurkat cells were engineered to express an anti-CD19 CAR (left) or the same with addition of the zinc finger degron from IKZF3 (Degradable CAR, right) and exposed to 1 μM lenalidomide or vehicle control overnight. UTD, untransduced. **(C)** Schematic of the ON-switch split CARs incorporating a lenalidomide-inducible dimerization domain composed of portions of CRBN in one subunit and IKZF3 in the other and their activation by lenalidomide or other thalidomide analogs. **(D)** Jurkat cells were engineered to express a conventional CAR (CAR) or a split CAR, co-cultured overnight with either K562 cells or K562 cells engineered to express CD19 and 1 μM lenalidomide or vehicle control, and the percentage of cells positive for the early activation marker CD69 was quantified by flow cytometry. Data representative of 1 of 2 independent experiments performed in technical duplicate (**B**) or triplicate (**D**). Error bars indicate mean ± SD of triplicate wells. Two-tailed *t*-test, #### $P < 0.00005$; ns, $P > 0.05$.

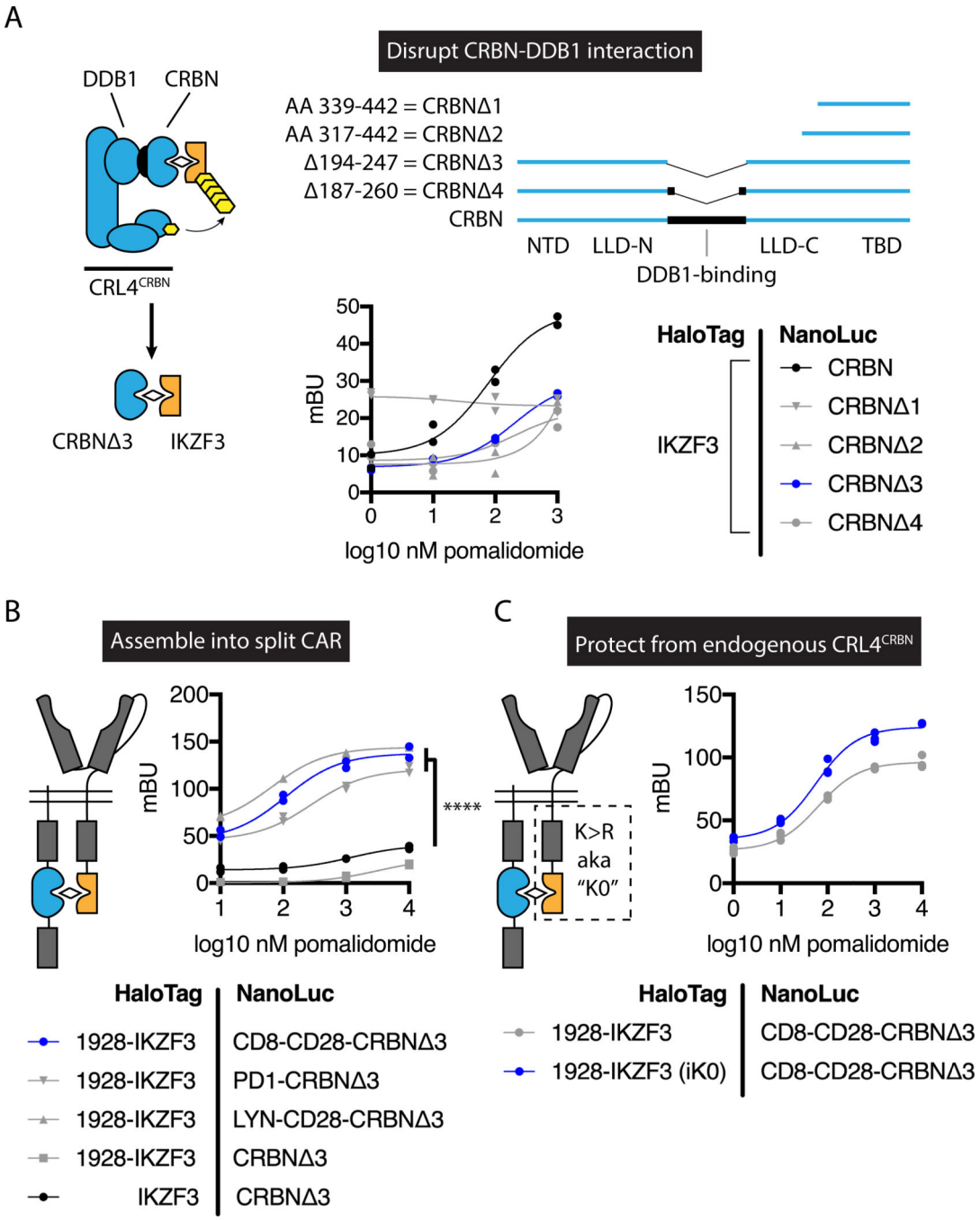

Fig. 2: Engineering of a lenalidomide-inducible dimerization system and ON-switch split CAR.

Bioluminescence resonance energy transfer (BRET) was used to measure the association between the indicated NanoLuc luciferase and HaloTag fusion proteins in 293T cells. **(A)** BRET analysis of IKZF3 interaction with CRBN deletion variants. IKZF3 = amino acids (AA) 130–189 of IKZF3. NTD, N-terminal domain; LLD-N, Lon-like domain (N-terminal portion); LLD-C, Lon-like domain (C-terminal portion); TBD, thalidomide-binding domain. **(B)** BRET analysis of IKZF3-CRBNΔ3 incorporated into cell surface-localized fusion proteins. 1928 = FMC63 scFv – CD28 hinge, transmembrane, and costimulatory domains.

CD8-CD28 = CD8 hinge and transmembrane domain and CD28 co-stimulatory domain. PD1 = PD1 transmembrane and cytoplasmic domain. LYN-CD28 = LYN myristoylation and palmitoylation motif – CD28 costimulatory domain. MG132 was included in experiments **A** and **B**. **(C)** BRET analysis of CD8-CD28-CRBNΔ3 and 1928-IKZF3 with or without intracellular Lys → Arg mutations (iK0). mBU, miliBRET units. Individual values and nonlinear regression are shown. Data represent one independent experiment performed in technical duplicate. Two-way ANOVA, **** $P < 0.0001$.

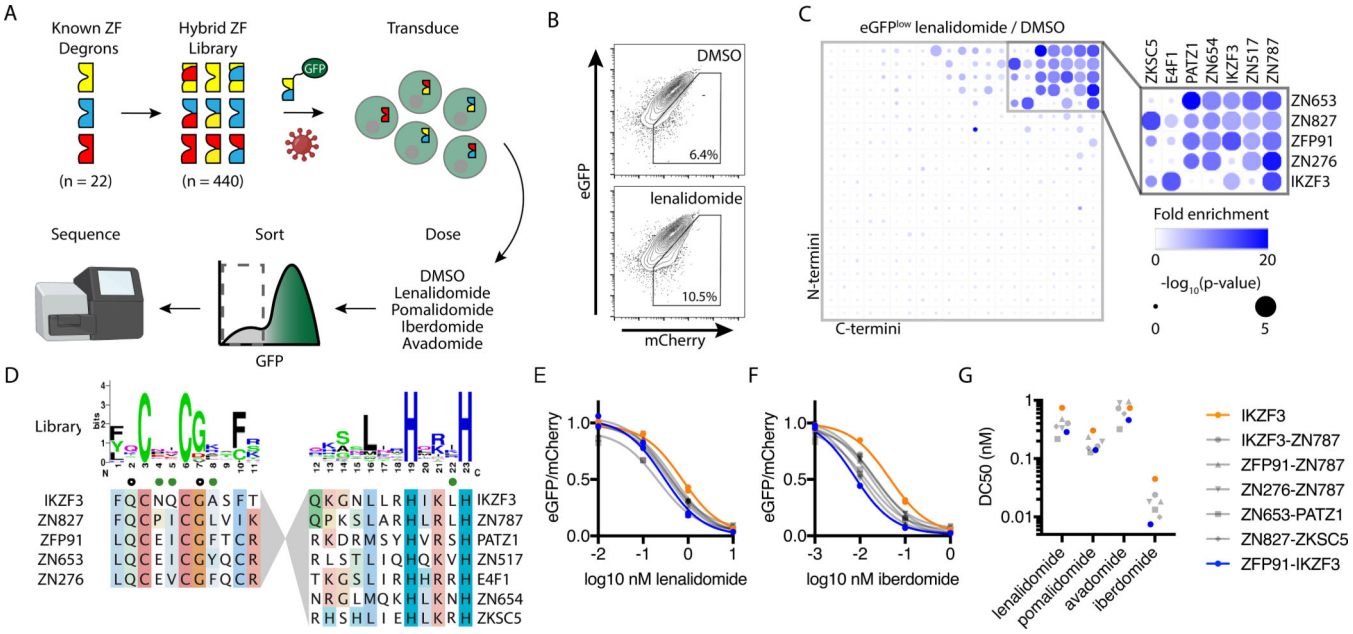

Fig. 3: A screen of 440 hybrid zinc fingers identifies “super-degrons” targeted by subnanomolar concentrations of thalidomide analogs.

(A) Schematic for the design and screening of a hybrid zinc finger (ZF) library encoded in a eGFP-tagged protein degradation reporter lentivector that also expressed mCherry as a control for lentivector transgene expression. Jurkat cells were transduced with the lentivirus library and then exposed to various thalidomide analogs or vehicle control (DMSO). FACS was used to isolate eGFP^{low} cells, and next-generation sequencing (NGS) was used to quantify the relative abundance of each sequence with and without drug treatment. **(B)** Flow plot for Jurkat cells transduced with the eGFP-tagged zinc finger library after overnight incubation with 1 μM lenalidomide or vehicle control. **(C)** Fold-enrichment of sequencing read counts (lenalidomide/DMSO, scale 0 – 20) and corresponding empirical rank-sum test *P* values (0 – 5). Average of nine replicates is presented (library of triplicate barcoded sequences assayed with triplicate independent biologic replicates). **(D)** Sequence features for N- and C-terminal domains present in top candidate super-degrons. Amino acid positions with prior crystallographic evidence of side-chain interactions with pomalidomide (open circle) or CRBN (green circle) are noted. Jurkat cells were engineered to express the indicated zinc finger constructs and treated with various thalidomide analogs. **(E and F)** Degradation of GFP-tagged zinc fingers was assessed by flow cytometry from the vehicle control-normalized eGFP/mCherry fluorescence ratio in Jurkat cells after treatment with lenalidomide (E) or iberdomide (F). Individual values and nonlinear regression are shown. Experiment was performed once in technical duplicate. **(G)** Nonlinear regression was used to calculate half maximal degradation concentration (DC50) values for zinc finger degradation by each drug.

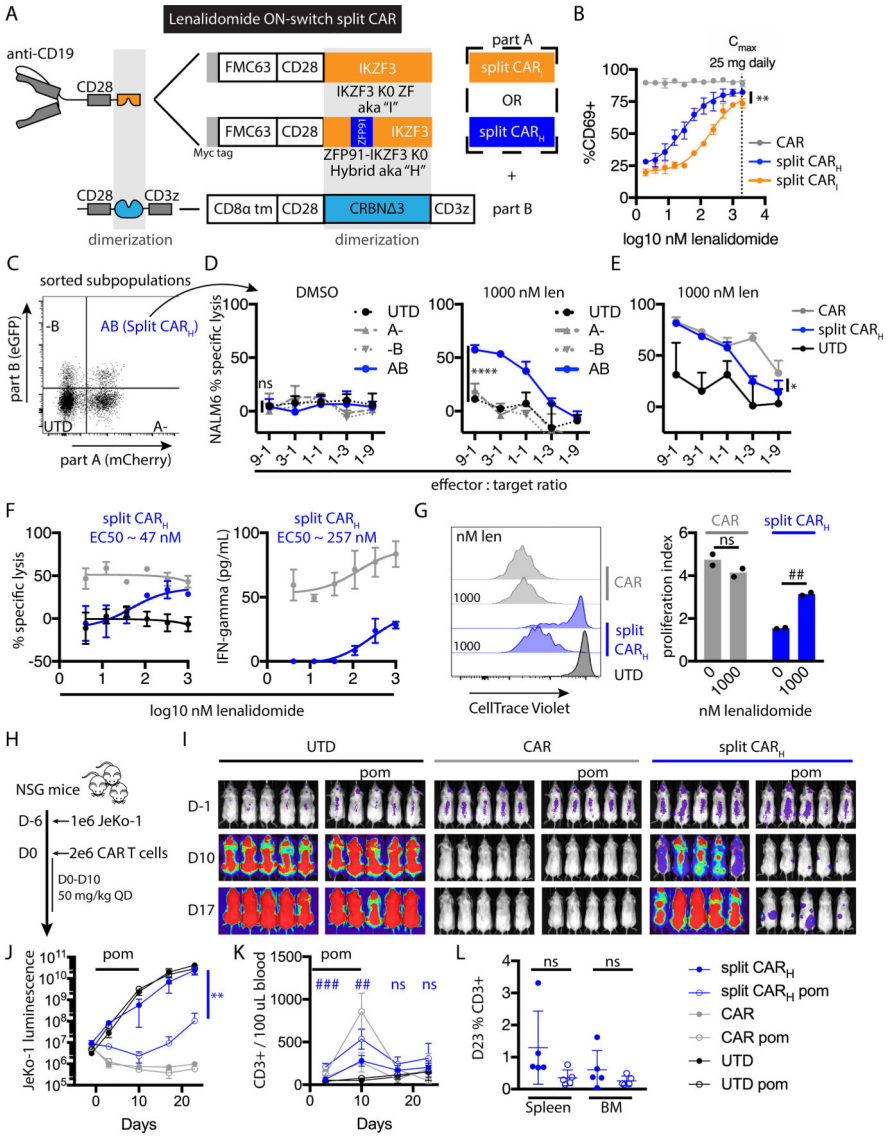

Fig. 4: Lenalidomide ON-switch control of split CAR function.

(A) Schematic of split CAR constructs. Each split CAR is composed of the indicated antigen-binding part (part A) and the CD3z-containing part (part B). In part A, the dimerization module is encoded either by amino acids (AAs) 130–189 of IKZF3, including the minimal drug- and CRBN-interacting zinc finger (AAs 146–168) and adjacent sequences that further enhance CRBN binding (split CAR_I), or by the ZFP91-IKZF3 hybrid zinc finger, which incorporates ZFP91 AAs 450–460 in place of IKZF3 AAs 146–156 (split CAR_H). The intracellular domains of each part A are protected from $CRL4^{CRBN}$ ubiquitination by Lys→ Arg "K0" substitutions. In part B, CRBNΔ3 is a deletion variant lacking the DDB1-interacting domain from AAs 194–247. CAR indicates the second generation receptor FMC63-CD28-CD3z. To detect transduced cells by flow cytometry, part A includes a P2A element followed by mCherry, and part B includes in-frame eGFP. **(B)** Percent of CD69-positive Jurkat CAR T cells after overnight coculture with K562-CD19 cells and a range of lenalidomide concentrations. The maximum plasma concentration for once daily 25 mg

lenalidomide in multiple myeloma patients is indicated by the dotted line. **(C)** FACS purification of the indicated populations of primary T cells six days after transduction with lentivectors encoding parts A and B of split CAR_H. **(D)** Cytotoxic activity of each sorted cell population after overnight coculture with NALM6 target cells at the indicated effector:target ratios and lenalidomide or vehicle control. The comparison of AB versus UTD (untransduced) control cells is noted. **(E)** NALM6 cytotoxic activity of split CAR_H versus CAR and UTD. **(F)** Cytotoxic activity or IFN-γ concentration (measured by bead array) from the indicated CAR T cells after overnight coculture with an equal number of NALM6 cells and a range of lenalidomide concentrations. **(G)** CAR T cell proliferation after 5 days of coculture with NALM6 cells. For in vitro experiments, error bars indicate mean ± SD of triplicate wells in all cases except proliferation, which shows individual values and means of duplicate wells. **(H)** Experimental design of in vivo study. **(I)** Bioluminescence flux (photons/s) of whole mice in each group, indicating tumor burden. **(J)** Bioluminescence at representative time points. ANOVA of split CAR with versus without lenalidomide is indicated. **(K)** Blood T cell quantification at representative time points. *t*-tests of split CAR with versus without lenalidomide treatment at each timepoint are indicated. **(L)** Percent of human CD3+ cells in the spleen and bone marrow at day 23 (D23). For in vivo experiments, error bars indicate mean ± SD of pentuplicate groups. Data represent 1 of 2 independent experiments. Two-way ANOVA, * $P < 0.05$; ** $P < 0.005$; **** $P < 0.0001$; ns, $P > 0.05$. Two-way *t*-test, ## $P < 0.005$; ### $P < 0.0005$; ns, $P > 0.05$.

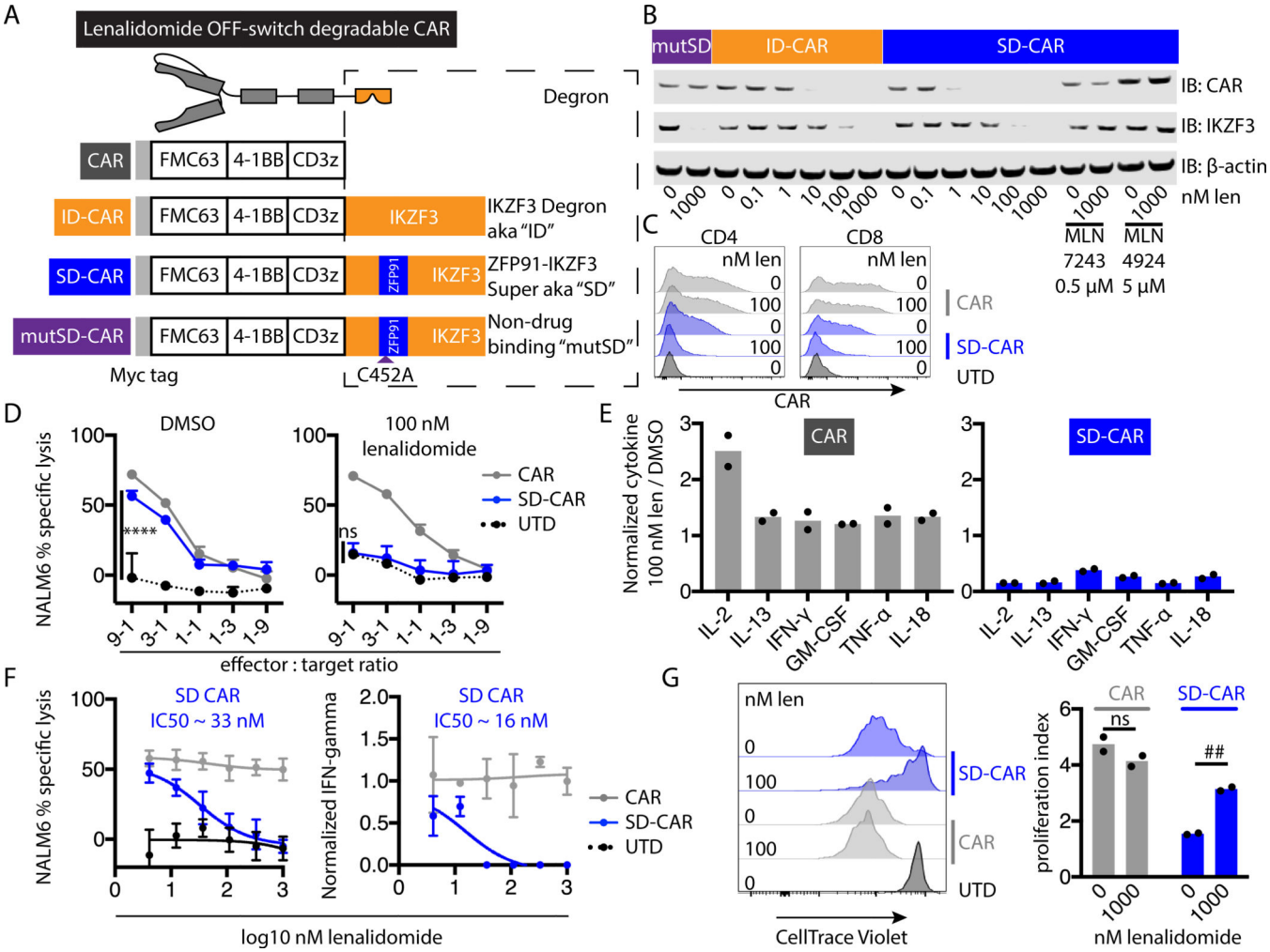

Fig. 5: Subtherapeutic lenalidomide concentrations trigger super-degron OFF-switch degradable CARs with 4–1BB and CD3z signaling domains.

(A) Degron-containing CAR constructs. The IKZF3 degron (ID) is encoded by the fragment of IKZF3 from amino acid (AA) 130–189. The ZFP91-IKZF3 super degron (SD) incorporates ZFP91 AAs 450–460 in place of IKZF3 AAs 146–156. The mutated super-degron (mutSD) has a C452A mutation in the ZFP91 fragment that abolishes drug binding. **(B)** Jurkat cells expressing the indicated CARs were drug treated overnight and then analyzed by Western blot for CAR (using an antibody recognizing CD3z) and other specified targets. **(C)** Surface CAR abundance (detected with antibody recognizing the Myc tag) on CD4+ and CD8+ CAR T cells after overnight incubation with lenalidomide or vehicle control. UTD, untransduced. (**D**) Cytotoxic activity of primary human CAR T cells after overnight coculture with NALM6 target cells and lenalidomide or vehicle control. **(E)** Cytokine concentrations in coculture supernatants measured by bead array (9:1 CAR T:NALM6 ratio). **(F)** Cytotoxic activity of or IFN-γ secreted from the indicated CAR T cells after overnight coculture with an equal number of NALM6 cells and a range of lenalidomide concentrations. IFN-γ was normalized to the concentration without lenalidomide for each construct. **(G)** CAR T cell proliferation after 5 days of coculture with NALM6 cells. Data represent 1 of 2 independent experiments. Error bars indicate mean ±

SD of triplicate wells. Individual values and means are shown for multiplexed cytokine analysis and proliferation, which were performed in duplicate. Two-way ANOVA, **** $P < 0.0001$; ns, $P > 0.05$. Two-way *t*-test, ## $P < 0.005$; ns, $P > 0.05$.

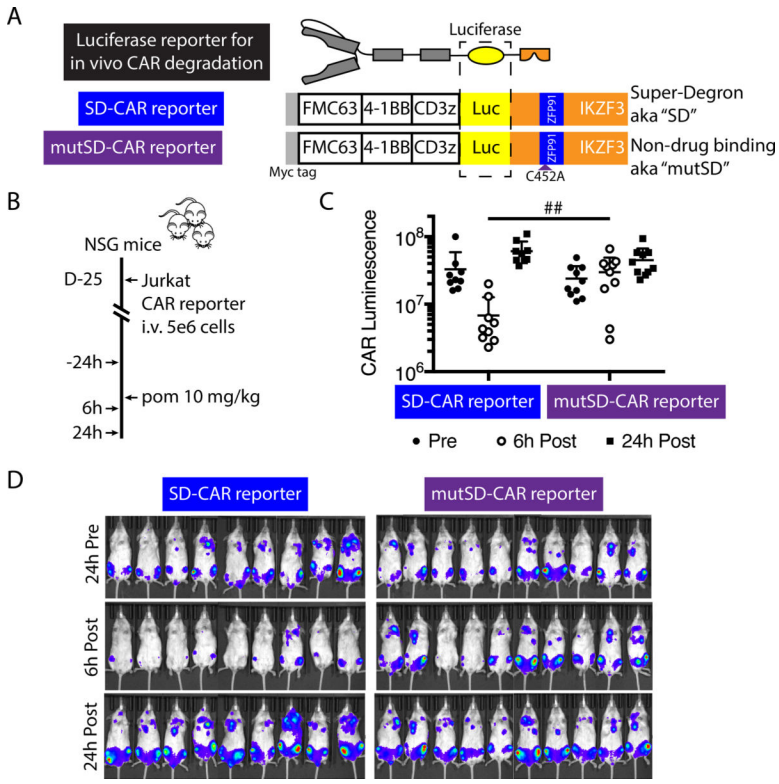

Fig. 6: Reversible lenalidomide OFF-switch control of a degradable CAR in vivo.

(A) Schematic of luciferase-tagged CAR constructs. **(B)** Experimental design for in vivo CAR depletion analysis: NSG mice were injected intravenously with 5×10^6 Jurkat cells expressing the SD or mutSD CAR reporter; after engraftment, bioluminescent imaging was performed before and after one dose of 10 mg/kg pomalidomide administered by oral gavage. **(C)** Luminescence 24 hours before, 6 hours after, and 24 hours after pomalidomide. Two-way *t*-test, ## $P < 0.005$ at 6 hours post, $P > 0.05$ at other timepoints. **(D)** Bioluminescence flux (photons/s) of whole mice in each group, indicating CAR protein abundance. Data represent 1 of 2 independent experiments.

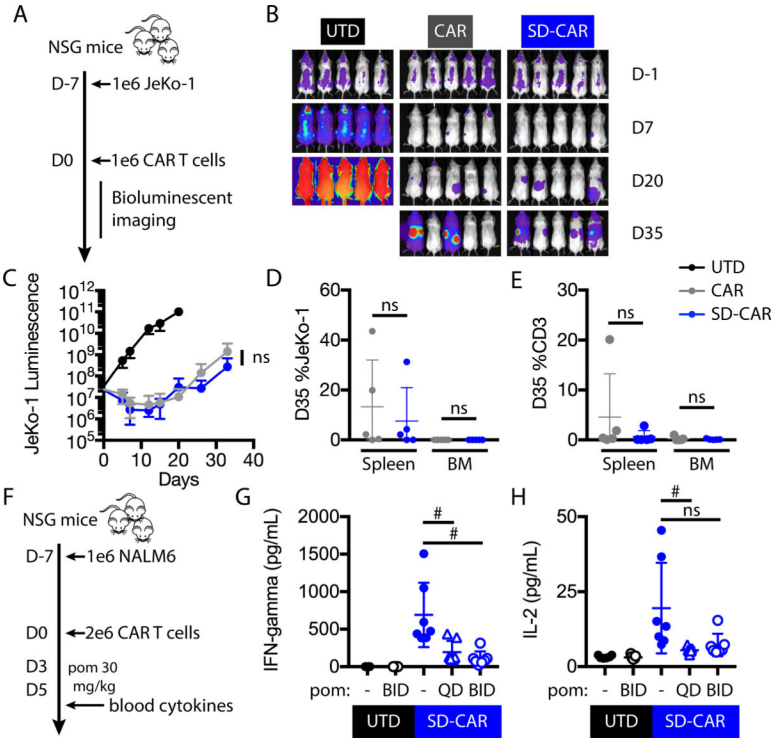

Fig. 7: Degradable CAR function and cytokine OFF-switch in vivo.

(A) Experimental design: NSG mice were injected intravenously with 1 × 10^6 GFP+/ luciferase+ JeKo-1 tumor cells. At day 0, mice were randomly assigned on the basis of tumor burden to receive 1 × 10^6 untransduced, CAR, or SD-CAR T cells. **(B)** Bioluminescence of whole mice in each group, indicating tumor burden. **(C)** Bioluminescence flux (photons/s) at representative time points. Two-way ANOVA, ns, $P > 0.05$. **(D, E)** Percent of JeKo-1 and human CD3+ cells in the bone marrow and spleen at day 35 (D35). Error bars indicate mean ± SD of pentuplicate groups. **(F)** Experimental design for in vivo CAR T cell cytokine release analysis: NSG mice were injected intravenously with 1 × 10^6 NALM6 cells. At day 0, mice were randomly assigned on the basis of tumor burden to receive 2 × 10^6 untransduced or SD-CAR T cells. From days 3 – 5, mice received no treatment, once daily, or twice daily 30 mg/kg pomalidomide by oral gavage. On the afternoon of day 5, serum was analyzed by bead array for human cytokines. **(G, H)** Serum IFN-γ and IL-2 concentrations. QD, daily. BID, twice daily. Two-way *t*-test, # $P < 0.05$; ns, $P > 0.05$.